

# Synthesis, crystal structure and magnetic properties of a mononuclear and a ferromagnetically coupled dinuclear nickel(II) complex derived from a hexadentate Schiff base ligand

Sushama Sain<sup>a</sup>, Soumitra Bid<sup>a</sup>, A. Usman<sup>b</sup>, Hoong-Kun Fun<sup>b</sup>, Guillem Aromí<sup>c,\*</sup>,  
Xavier Solans<sup>d</sup>, Swapan K. Chandra<sup>\*,a,1</sup>

<sup>a</sup> Department of Chemistry, The University of Burdwan, Burdwan – 713104, India

<sup>b</sup> X-ray Crystallography Unit, School of Physics, Universiti Sains Malaysia, 11800 USM, Penang, Malaysia

<sup>c</sup> Departament de Química Inorgànica, Facultat de Química, Universitat de Barcelona, Diagonal 647, 08028 Barcelona, Spain

<sup>d</sup> Departament de Cristal·lografia i Mineralogia, Universitat de Barcelona, Martí i Franquès s/n, 08028 Barcelona, Spain

Received 3 February 2005; received in revised form 21 April 2005; accepted 11 May 2005

Available online 16 June 2005

## Abstract

Reactions with Ni<sup>II</sup> of a hexadentate Schiff base ligand, L, prepared from the reaction of 2-benzoylpyridine with *N,N'*-bis-(3-aminopropyl) ethylenediamine in the 2:1 molar ratio are reported. Mixing of this ligand with Ni(NO<sub>3</sub>)<sub>2</sub> affords the mononuclear complex [NiL](NO<sub>3</sub>)<sub>2</sub> (**1**), whereas the presence of NaN<sub>3</sub> in the reaction system leads to the formation of the dinuclear complex [Ni<sub>2</sub>(L)(N<sub>3</sub>)<sub>4</sub>] (**2**). Both adducts have been characterized by X-ray crystallography revealing distorted octahedral NiN<sub>6</sub> coordination environments around the Ni<sup>II</sup> centers. The dinuclear complex contains terminal and end-on bridging azido ligands and displays Ni–N–Ni bridge angles of 101.1(2)° and 101.6(2)° and an intramolecular Ni···Ni separation of 3.330(1) Å. The μ-N<sub>3</sub><sup>−</sup> bridges mediate ferromagnetic magnetic exchange interactions between the Ni<sup>II</sup> centers of **2**, leading to an *S* = 2 ground state. Fitting of bulk magnetization data provided the coupling constant *J* = +20.96 cm<sup>3</sup> K mol<sup>−1</sup> (in the *H* = −2*J**S*<sub>1</sub> · *S*<sub>2</sub> convention for the Heisenberg Spin Hamiltonian), as well as the parameters *g* = 2.17, *D* = 0.69 cm<sup>−1</sup> and TIP = 622 × 10<sup>−6</sup> cm<sup>3</sup> mol<sup>−1</sup>.

© 2005 Elsevier B.V. All rights reserved.

**Keywords:** Nickel; Magnetism; Ferromagnetic coupling; Azide ligands

## 1. Introduction

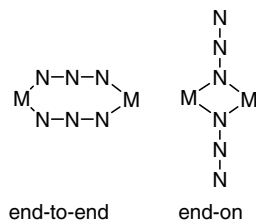
One of the areas that most have stimulated the synthesis of polynuclear coordination complexes is that of molecular magnetism. Many synthetic strategies have been developed to this end, and all them have in common the use of bridging ligands for the assembly

of various transition metal ions into molecular species. Such ligands span from simple mono- or didentate ions (Cl<sup>−</sup>, HO<sup>−</sup>, RO<sup>−</sup>, N<sub>3</sub><sup>−</sup>, RCOO<sup>−</sup>, etc.) [1,2], all the way to very elaborate multidentate molecules [3,4]. Very often, judicious or serendipitous combinations of more than one species lying on opposite sides of that spectrum are used [5]. The use of the azido ion has been very beneficial in this respect [6], thanks to the versatility of its bridging modes and because it has shown the ability to facilitate efficiently the magnetic exchange between the spin carriers that it links. The most common bridging modes of N<sub>3</sub><sup>−</sup> are (Scheme 1) the end-on ( $\eta^1 : \mu\text{-N}_3^-$ ) [7–9] and the end-to-end ( $\eta^{1,3} : \mu\text{-N}_3^-$ ) fashion [10–12],

\* Corresponding author. Tel.: +34 934021271; fax: +34 934907725.

E-mail addresses: [guillem.aromi@qi.ub.es](mailto:guillem.aromi@qi.ub.es) (G. Aromí), [dr\\_swapan@sify.com](mailto:dr_swapan@sify.com) (S.K. Chandra).

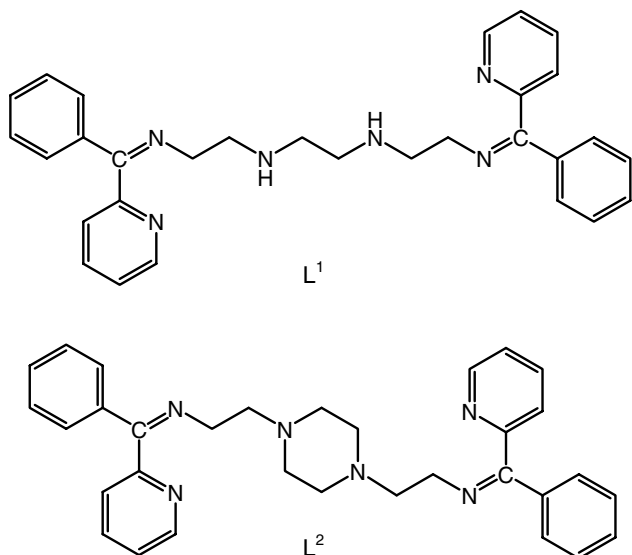
<sup>1</sup> Present address: Department of Chemistry, Visva Bharati, Santiniketan 731 235, India.



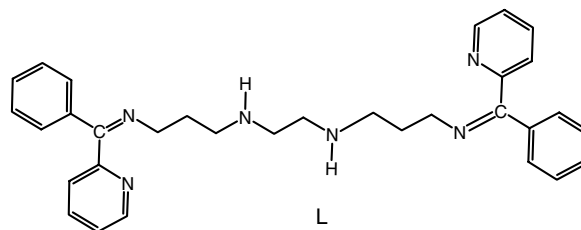
Scheme 1.

which generally lead to ferro- and antiferromagnetic interactions, respectively.

Some of us have recently reported on the reactivity toward  $\text{Ni}^{\text{II}}$  of a hexadentate Schiff base-type ligand (Scheme 2),  $\text{L}^1$ , where the central tetradentate part is based on a triethylenetetraamine moiety [13]. It was found that the reaction of  $\text{L}^1$  with  $\text{Ni}(\text{ClO}_4)_2$  lead to the mononuclear complex  $[\text{NiL}^1](\text{ClO}_4)_2$ , whereas the presence of  $\text{NaN}_3$  in the reaction system conduced to the formation of the dinuclear complex  $[\text{Ni}_2\text{L}^2(\text{N}_3)_4]$ , where  $\text{L}^2$  is a hexadentate ligand related to  $\text{L}^1$ , resulting from in situ transformation of the latter (Scheme 2). The same reaction using  $\text{Ni}(\text{NO}_3)_2$  produced the same neutral dinuclear compound. We report here the analogous reactivity of a very similar hexadentate ligand, ( $\text{L}$ , Scheme 3) with a central moiety originating from the  $N,N'$ -bis-(3-aminopropyl)ethylenediamine group. The additional methylene groups within the backbone of  $\text{L}$  provide the ligand with more flexibility, potentially inducing to changes of reactivity with respect to  $\text{L}^1$ . In the absence of other co-ligands, a mononuclear complex,  $[\text{NiL}](\text{NO}_3)_2 \cdot \text{H}_2\text{O}$  ( $\mathbf{1} \cdot \text{H}_2\text{O}$ ), is isolated from the reaction between  $\text{L}$  and  $\text{Ni}(\text{NO}_3)_2$ . The addition of  $\text{NaN}_3$  to the mixture, however, leads to the formation of the dinuclear bis( $\mu$ -azido) complex  $[\text{Ni}_2(\text{L})(\text{N}_3)_4] \cdot \text{CH}_3\text{CN}$  ( $\mathbf{2} \cdot \text{CH}_3\text{CN}$ ), where the ligand  $\text{L}$  re-



Scheme 2.



Scheme 3.

mains unchanged. Both complexes have been crystallographically characterized and their magnetic properties are discussed.

## 2. Experimental

### 2.1. Synthesis

$N,N'$ -bis-(3-aminopropyl)ethylenediamine, 2-benzoyl pyridine and sodium azide were purchased from Lancaster Chemical Company Inc. and were used as received. All other solvents and chemicals were of analytical grade.

#### 2.1.1. Preparation of ligand

$N,N'$ -bis-(3-aminopropyl)ethylenediamine (0.87 g, 5 mmol) and 2-benzoylpyridine (1.83 g, 10 mmol) were refluxed in dehydrated ethanol (15 mL) for 15 h. The hexadentate ligand ( $\text{L}$ ) was isolated after evaporating the solvent and was recrystallized from water/ethanol. The product was isolated as a brown wax after drying in vacuum over  $\text{P}_4\text{O}_{10}$ . The yield was 2.05 g (~81%). *Anal.* Calc. for  $\text{C}_{32}\text{H}_{36}\text{N}_6$  ( $\text{L}$ ): C, 76.12; H, 7.18; N, 16.60. Found: C, 76.02; H, 7.05; N, 16.48%. IR ( $\text{cm}^{-1}$ ): 1617, 1591, 1453, 1329, 993, 800, 697.

#### 2.1.2. Preparation of $[\text{Ni}(\text{L})](\text{NO}_3)_2$ ( $\mathbf{1}$ )

To an acetonitrile solution ( $5 \text{ cm}^3$ ) of  $\text{Ni}(\text{NO}_3)_2 \cdot 6\text{H}_2\text{O}$  (0.146 g, 0.5 mmol) was added ligand  $\text{L}$  (0.252 g, 0.5 mmol) dissolved in acetonitrile (10 mL) over a period of 10 min. The resulting dark red solution was then filtered and left for slow evaporation. After 3–4 days deep red crystals of  $\mathbf{1} \cdot \text{H}_2\text{O}$  were obtained (0.15 g, ~42% yield) which were suitable for X-ray crystallography. These were collected by filtration and dried in vacuum. *Anal.* Calc. for  $\text{C}_{32}\text{H}_{36}\text{N}_8\text{O}_6\text{Ni}$  ( $\mathbf{1}$ ): C, 54.60; H, 5.16; N, 15.93; Ni, 8.06. Found: C, 54.38; H, 5.01; N, 15.72; Ni, 7.98%. IR ( $\text{cm}^{-1}$ ): 1617, 1592, 1384, 1020, 945, 800, 778, 751, 707, 684.

#### 2.1.3. Preparation of $[\text{Ni}_2(\text{L})(\text{N}_3)_4]$ ( $\mathbf{2}$ )

To an acetonitrile solution ( $5 \text{ cm}^3$ ) of  $\text{Ni}(\text{NO}_3)_2 \cdot 6\text{H}_2\text{O}$  (0.146 g, 0.5 mmol) was added ligand  $\text{L}$  (0.126 g, 0.25 mmol) of in acetonitrile (10 mL) over a period of 10 min. To the resulting brown solution, an aqueous solution (2 mL) of sodium azide (0.065 g, 1.0 mmol)

was added slowly. The solution was then filtered and the insoluble yellow precipitate (proven by IR not to be  $\text{NaNO}_3$ ) was discarded. The filtrate was left for slow evaporation and after 3–4 days deep brown crystals of  $2 \cdot \text{CH}_3\text{CN}$  were obtained (0.06 g, ~30% yield). These were collected by filtration and dried in vacuum. *Anal.* Calc. for  $\text{C}_{32}\text{H}_{36}\text{N}_{18}\text{Ni}_2$ : C, 48.64; H, 4.59; N, 31.91; Ni, 14.85. Found: C, 48.49; H, 4.41; N, 31.76; Ni, 14.62%. IR ( $\text{cm}^{-1}$ ): 2071, 2039, 1617, 1591, 1442, 1332, 1078, 1037, 795, 702.

**Caution.** Azido complexes are potentially explosive especially in presence of organic ligands. Therefore, these compounds must be handled with care and prepared only in small amounts.

## 2.2. Physical measurements

Elemental analyses for carbon, hydrogen and nitrogen were performed using a Perkin–Elmer 2400II elemental analyzer. Nickel contents were determined gravimetrically as the nickel dimethyl glyoximate complex. Variable temperature magnetic susceptibility data were obtained with a Quantum Design MPMS5 SQUID spectrophotometer. Pascal's constants were utilized to estimate diamagnetic corrections to the molar paramagnetic susceptibility. IR spectra ( $4000\text{--}400\text{ cm}^{-1}$ ) were taken at 298 K using a JASCO FT/IR-420 spectrometer.

## 2.3. Crystal structure determinations and refinement

A crystal of  $1 \cdot \text{H}_2\text{O}$  was mounted on an area detector CCD diffractometer equipped with a graphite monochromated Mo  $\text{K}\alpha$  radiation source. This crystal was twinned with a twin law mirror plane perpendicular to the  $c$ -axis. The molar fraction of each twin component was 0.275(14) and 0.725(14), respectively, and the results of the major component are given. Intensity data were collected in the  $\omega - 2\theta$  scan mode. Lorentz and polarization corrections were made. The non-hydrogen atoms were refined anisotropically. The enhanced thermal motion of atoms C9, C10, C11, as well as that of the O atoms of the  $\text{NO}_3^-$  ions is likely caused by some type of disorder that could not be resolved. The aliphatic and aromatic H-atoms have been calculated and refined using a riding model, whereas the amine H-atoms were localized through difference synthesis. The H-atoms of  $\text{H}_2\text{O}$  molecules could not be localized. Two of the  $\text{NO}_3^-$  groups are involved in H-bonds with amine hydrogen atoms from both complex cations, respectively, forming 1-D networks along the crystallographic  $b$  direction (not shown). The other two  $\text{NO}_3^-$  anions are located at interstitial positions.

Data collection on a suitable crystal of  $2 \cdot \text{CH}_3\text{CN}$  were performed with a Siemens SMART CCD area

detector equipped with a graphite monochromated Mo  $\text{K}\alpha$  radiation source. Intensity data were collected in the  $\omega - 2\theta$  scan mode. The data were corrected for Lorentz, polarization and absorption effects, the latter using SADABS. The non hydrogen atoms were refined anisotropically. Hydrogen atoms were included but not refined. Both structures were solved with SHELXS97 and refined with SHELXL97 computer programs [14,15]. The crystal data and data collection details are collected in Table 1.

## 3. Results and discussion

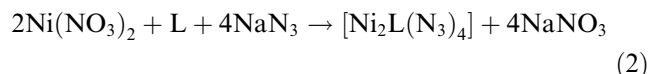
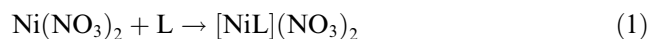
### 3.1. Synthesis

The hexadentate ligand was made adopting a procedure modified from that for the related ligand  $\text{L}^1$  [13]. Thus, L could be easily obtained via the condensation taking place by refluxing  $N,N'$ -bis-(3-aminoethyl)-ethylenediamine and 2-benzoylpyridine in the 1:2 molar ratio in dehydrated ethanol. The reaction of L with one equivalent of  $\text{Ni}(\text{NO}_3)_2 \cdot 6\text{H}_2\text{O}$  in aqueous acetonitrile produced a dark red colored crystalline complex of composition  $[\text{NiL}](\text{NO}_3)_2 \cdot \text{H}_2\text{O}$  ( $1 \cdot \text{H}_2\text{O}$ ). Thus, the flexibility of the ligand allows itself to wrap around the metallic center and saturate with its six donor atoms

Table 1  
Crystal data for  $1 \cdot \text{H}_2\text{O}$  and  $2 \cdot \text{CH}_3\text{CN}$

	$1 \cdot \text{H}_2\text{O}$	$2 \cdot \text{CH}_3\text{CN}$
Formula	$\text{Ni}_2\text{C}_{64}\text{H}_{76}\text{N}_{16}\text{O}_{14}$	$\text{Ni}_2\text{C}_{34}\text{H}_{39}\text{N}_{19}$
Formula weight	705.41	831.26
Space group	$Pca2_1$ (no. 29)	$P2_1/c$ (no. 14)
<i>Unit cell dimensions</i>		
$a$ (Å)	23.3761(12)	12.1292(16)
$b$ (Å)	9.6785(5)	10.8317(14)
$c$ (Å)	28.9032(15)	31.739(4)
$\alpha$ (°)	90	90
$\beta$ (°)	90	112.241(4)
$\gamma$ (°)	90	90
$V$ (Å <sup>3</sup> )	6539.2(6)	3859.6(9)
$Z$	8	4
$D_{\text{calc}}$ (g cm <sup>-3</sup> )	1.433	1.431
$F_{(000)}$	2944	1728
Crystal size (mm)	0.20 × 0.25 × 0.30	0.42 × 0.34 × 0.18
$\mu$ (Mo $\text{K}\alpha$ ) (mm <sup>-1</sup> )	0.654	1.029
$\lambda$ (Å)	0.71073	0.71073
Temperature (K)	100(2)	293(2)
$2\theta_{\text{max}}$ (°)	56.7	56.64
Reflections collected	44129	23246
Independent reflections	12036 ( $R_{\text{int}} = 0.0604$ )	9447 ( $R_{\text{int}} = 0.0308$ )
Reflections observed	10365	9447
[ $I > 2\sigma(I)$ ]		
Goodness-of-fit	1.036	1.101
$R; R_w$	0.0550; 0.1283	0.0947; 0.2360
Largest difference peak and hole (e Å <sup>-3</sup> )	0.649 and -0.325	0.939 and -1.256

all the positions of the common octahedral coordination geometry of Ni<sup>II</sup>. This reactivity is analogous to that of the previously reported similar ligand L<sup>1</sup>, which features only ethylene groups within its backbone. Of especial interest was the reactivity of L within the same reaction system in the presence of N<sub>3</sub><sup>-</sup>. A specific question to answer was whether L would undergo in situ transformation as observed with L<sup>1</sup> in the same conditions. On the contrary, mixing Ni(NO<sub>3</sub>)<sub>2</sub> · 6H<sub>2</sub>O, L and NaN<sub>3</sub> in aqueous acetonitrile medium using the 2:1:4 molar ratio afforded a deep brown product in form of crystals suitable for X-ray crystallography, identified as [Ni<sub>2</sub>L(N<sub>3</sub>)<sub>4</sub>] · CH<sub>3</sub>CN (**2** · CH<sub>3</sub>CN). Thus, the addition of N<sub>3</sub><sup>-</sup> allows the combined presence of a multidentate ligand and a small bridging group within a dinuclear species, with the metals featuring the same octahedral NiN<sub>6</sub> environment as in **1**. The above transformations are summarized in Eqs. (1) and (2).



### 3.2. IR spectroscopy

The IR spectrum of **2** exhibits two broad bands corresponding to the asymmetric stretching vibrations of the ligand N<sub>3</sub><sup>-</sup> at 2071 and 2039 cm<sup>-1</sup>, respectively, which are similar to those previously reported [9,16]. The stretching vibrations of the C=N bond of the Schiff base L are located at 1617 and 1591 cm<sup>-1</sup>, respectively.

### 3.3. Description of the structures

[Ni(L)](NO<sub>3</sub>)<sub>2</sub> · H<sub>2</sub>O (**1**). An ORTEP representation of the independent complex cations of **1** is shown in Fig. 1, whereas selected bond distances and angles are listed in Table 2. The crystal structure of **1** · H<sub>2</sub>O consists of two independent, but structurally equivalent, cationic molecules per asymmetric unit, with two non-coordinated NO<sub>3</sub><sup>-</sup> anions per molecule located in between these. The complex cation of Ni(1) displays C<sub>2</sub> molecular symmetry within a tolerance of 0.5 Å, which is not the case for the other complex. This difference is caused by small deviations in torsion angles, both molecules presenting otherwise essentially the same geometry. Each molecule features one Ni<sup>II</sup> center surrounded and chelated by one hexadentate ligand L which saturates the six positions of a distorted octahedral NiN<sub>6</sub> coordination environment through the formation of four fused chelate rings. Of these, two are planar, conjugated five-membered rings, whereas the other two comprise aliphatic carbons and are formed by six atoms that are far from lying in a plane. The coordination Ni–N distances span 2.079(3)–2.111(3) Å, whereas the ranges

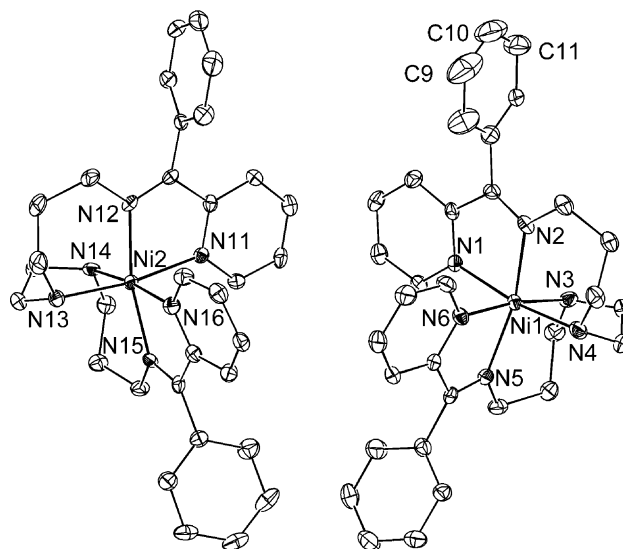


Fig. 1. Labeled ORTEP representation at 50% probability level of the crystallographically independent complex cations of [NiL](NO<sub>3</sub>)<sub>2</sub> (**1**). For clarity, the nitrate anions, crystallized water and hydrogen atoms are not shown.

of observed N–Ni–N angles are 166.8(1)–172.7(1)° (*trans*) and 78.4(1)–96.3(1)° (*cis*) degrees, respectively. Two of the NO<sub>3</sub><sup>-</sup> groups are involved in H-bonds with amine hydrogen atoms from both complex cations, respectively, forming 1-D networks along the crystallographic *b* direction (not shown). The other two NO<sub>3</sub><sup>-</sup> anions are located at interstitial positions. The shortest Ni · · · Ni distance within the lattice is 8.243 Å.

[Ni<sub>2</sub>(L)(N<sub>3</sub>)<sub>4</sub>] · CH<sub>3</sub>CN (**2**). The molecular structure of **2** is shown in Fig. 2 in form of an ORTEP representation. Table 3 includes a list of selected interatomic distances and bond angles. Complex **2** is a neutral dinuclear molecule of Ni<sup>II</sup> where the metals are chelated and connected by one hexadentate ligand, L, and further bridged by two end-on μ-N<sub>3</sub><sup>-</sup> groups. The latter are responsible for holding both metals in close proximity to each other (3.3299(13) Å). The distorted octahedral environment around each Ni<sup>II</sup> center is completed by one terminal monodentate N<sub>3</sub><sup>-</sup> ligand. The central [Ni<sub>2</sub>(μ-N)<sub>2</sub>] moiety of the complex lies on an almost perfect plane, the molecule showing a virtual C<sub>2</sub> axis of symmetry passing through the center of that plane and the midpoint of the ethylene group of L. The Ni–Ni bridging angles within this plane are 101.1(2)° and 101.6(2)°, respectively. The bridging azido ligands are significantly bent with respect to the planar core of the dimer (as gauged by the angles N8–N7–N13 and N14–N13–N7 of 147.18(5)° and 146.2(5)°, respectively) and point opposite from the side where the backbone of the multidentate ligand L is located. The coordination Ni–N distances in **2** range from 2.075(6) to 2.159(6) Å, whereas the N–Ni–N angles are in the ranges

Table 2  
Selected interatomic distances (Å) and bond angles (°) for **1** · H<sub>2</sub>O

Ni(1)–N(2)	2.085(3)
Ni(1)–N(4)	2.092(3)
Ni(1)–N(5)	2.101(3)
Ni(2)–N(11)	2.079(3)
Ni(2)–N(14)	2.088(3)
Ni(2)–N(15)	2.098(3)
Ni(1)–N(3)	2.087(4)
Ni(1)–N(6)	2.093(3)
Ni(1)–N(1)	2.111(3)
Ni(2)–N(13)	2.085(3)
Ni(2)–N(12)	2.098(3)
Ni(2)–N(16)	2.106(3)
N(2)–Ni(1)–N(3)	93.51(14)
N(3)–Ni(1)–N(4)	84.43(15)
N(3)–Ni(1)–N(6)	93.52(14)
N(2)–Ni(1)–N(5)	167.37(14)
N(4)–Ni(1)–N(5)	93.96(13)
N(2)–Ni(1)–N(1)	78.45(13)
N(4)–Ni(1)–N(1)	93.92(13)
N(2)–Ni(1)–N(4)	95.38(13)
N(2)–Ni(1)–N(6)	92.29(13)
N(4)–Ni(1)–N(6)	172.17(13)
N(3)–Ni(1)–N(5)	95.85(13)
N(6)–Ni(1)–N(5)	78.70(13)
N(3)–Ni(1)–N(1)	171.62(14)
N(6)–Ni(1)–N(1)	89.17(13)
N(5)–Ni(1)–N(1)	92.45(13)
N(11)–Ni(2)–N(14)	91.38(13)
N(11)–Ni(2)–N(12)	78.78(13)
N(14)–Ni(2)–N(12)	94.83(12)
N(13)–Ni(2)–N(15)	96.32(13)
N(12)–Ni(2)–N(15)	166.80(13)
N(13)–Ni(2)–N(16)	95.24(14)
N(12)–Ni(2)–N(16)	92.48(12)
N(11)–Ni(2)–N(13)	171.49(13)
N(13)–Ni(2)–N(14)	84.70(14)
N(13)–Ni(2)–N(12)	93.99(14)
N(11)–Ni(2)–N(15)	91.49(12)
N(14)–Ni(2)–N(15)	94.31(13)
N(11)–Ni(2)–N(16)	89.62(13)
N(14)–Ni(2)–N(16)	172.67(13)
N(15)–Ni(2)–N(16)	78.41(12)

Table 3  
Selected interatomic distances (Å) and bond angles (°) for **2** · MeCN

Ni(1)–N(1)	2.118(7)
Ni(1)–N(6)	2.091(6)
Ni(1)–N(13)	2.144(6)
Ni(2)–N(2)	2.124(7)
Ni(2)–N(4)	2.124(7)
Ni(2)–N(10)	2.079(6)
Ni(1)–N(5)	2.117(7)
Ni(1)–N(7)	2.152(6)
Ni(1)–N(16)	2.085(7)
Ni(2)–N(3)	2.075(6)
Ni(2)–N(7)	2.159(6)
Ni(2)–N(13)	2.150(6)
Ni(1)···Ni(2)	3.3299(13)
N(1)–Ni(1)–N(5)	169.7(2)
N(1)–Ni(1)–N(7)	92.0(2)
N(1)–Ni(1)–N(16)	89.6(3)
N(5)–Ni(1)–N(7)	94.0(2)
N(5)–Ni(1)–N(16)	85.5(3)
N(6)–Ni(1)–N(13)	167.7(2)
N(7)–Ni(1)–N(13)	78.7(2)
N(13)–Ni(1)–N(16)	93.8(3)
N(2)–Ni(2)–N(4)	170.2(2)
N(2)–Ni(2)–N(10)	89.3(3)
N(3)–Ni(2)–N(4)	94.0(2)
N(3)–Ni(2)–N(10)	95.4(2)
N(4)–Ni(2)–N(7)	91.9(2)
N(4)–Ni(2)–N(13)	93.8(2)
N(7)–Ni(2)–N(13)	78.4(2)
Ni(1)–N(7)–Ni(2)	101.1(2)
N(1)–Ni(1)–N(6)	77.6(2)
N(1)–Ni(1)–N(13)	97.5(2)
N(5)–Ni(1)–N(6)	94.1(2)
N(5)–Ni(1)–N(13)	91.9(2)
N(6)–Ni(1)–N(7)	90.1(2)
N(6)–Ni(1)–N(16)	97.4(3)
N(7)–Ni(1)–N(16)	172.5(3)
N(2)–Ni(2)–N(3)	77.9(2)
N(2)–Ni(2)–N(7)	97.0(2)
N(2)–Ni(2)–N(13)	92.0(2)
N(3)–Ni(2)–N(7)	169.7(2)
N(3)–Ni(2)–N(13)	92.8(2)
N(4)–Ni(2)–N(10)	85.9(3)
N(7)–Ni(2)–N(10)	93.4(2)
N(10)–Ni(2)–N(13)	171.8(2)
Ni(1)–N(13)–Ni(2)	101.7(2)

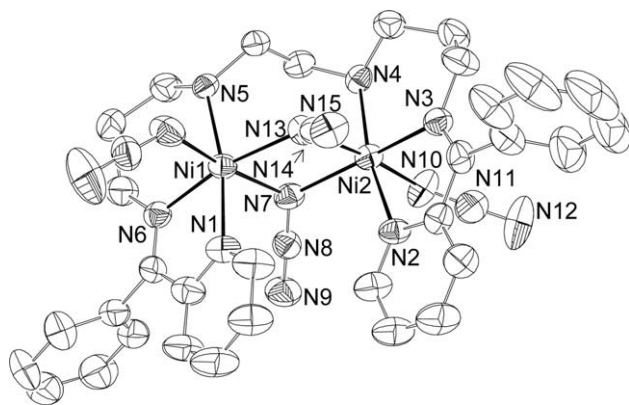


Fig. 2. Labeled ORTEP representation at 50% probability level of the complex  $[\text{Ni}_2(\text{L})(\text{N}_3)_4]$  (**2**). For clarity, the nitrate anions, crystallized acetonitrile and hydrogen atoms are not shown.

$77.6(2)$ – $97.5(2)^\circ$  and  $167.7(2)$ – $172.5(3)^\circ$  for pairs of N atoms in *cis* and *trans* positions, respectively.

### 3.4. Magnetic properties

The magnetic properties of **1** and **2** were evaluated by means of bulk magnetization measurements. The value of the product  $\chi_M T$  ( $\chi_M$  is the molar paramagnetic susceptibility) at 296 K ( $1.04 \text{ cm}^3 \text{ K mol}^{-1}$ ) for a powdered sample **1** is close to the spin-only value expected for a divalent nickel(II) compound comprising a  $^3A_2$  electronic state with  $g = 2$ . Variable temperature magnetic susceptibility measurements were performed on a polycrystalline sample of **2** in the 2–300 K temperature range, under a constant magnetic field of 7 kG. The

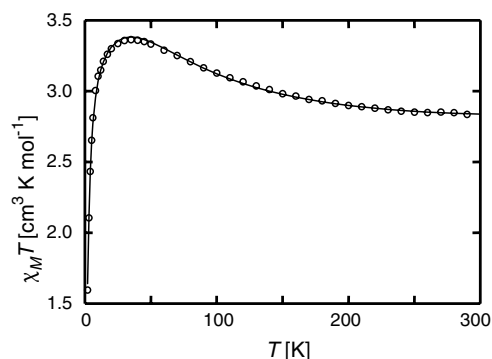


Fig. 3. Plot of experimental  $\chi_M T$  vs.  $T$ . The solid line is a fit to the experimental data (see text for details).

results are shown in Fig. 3 in form of a  $\chi_M T$  versus  $T$  plot. The product  $\chi_M T$  takes a value of  $2.83 \text{ cm}^3 \text{ K mol}^{-1}$  at room temperature, slightly higher than that expected for two independent  $\text{Ni}^{\text{II}}$  centers with  $g = 2.17$  (2.35). It increases gradually with cooling to reach a smooth maximum of  $3.36 \text{ cm}^3 \text{ K mol}^{-1}$ , at 35 K and decrease sharply down to  $1.60 \text{ cm}^3 \text{ K mol}^{-1}$  at 2 K. The expected value for a system with an isolated  $S = 2$  spin ground state and  $g = 2$  is  $3.53 \text{ cm}^3 \text{ K mol}^{-1}$ . This behavior shows that the intramolecular coupling within **2** is ferromagnetic, thus leading to the quintuplet as a ground state. The decrease of  $\chi_M T$  at low temperature is very likely to be caused by combination of zero field splitting of the ground state and intermolecular exchange interactions. Ginsberg et al. [17] pointed out that these two parameters are very strongly dependent of each other. The experimental data were fit to a theoretical  $\chi_M = f(T)$  expression derived from the Van Vleck equation for a dimer of two  $S = 1$  ions [18], modified in order to take into account the zero field splitting of the ground state [18], by introducing a  $D$  parameter (See supplementary material, Eq. S1). The best fit (Fig. 3, solid line) was obtained for  $J = 20.96 \text{ cm}^{-1}$ ,  $D = 0.69 \text{ cm}^{-1}$ ,  $g = 2.17$  and TIP (temperature independent paramagnetism) =  $622 \times 10^{-6} \text{ cm}^3 \text{ mol}^{-1}$ . Reduced magnetization,  $M/N\mu_B$ , measurements were also collected

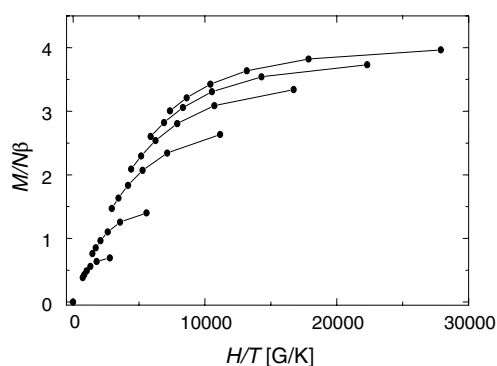


Fig. 4. Isofield reduced magnetization,  $M/N\beta$ , vs.  $H/T$  plots, recorded at various constant magnetic fields. The lines joining the data points are a guide to the eye.

in the 1.8–6.8 K temperature range at various constant magnetic fields. The resulting isofield  $M/N\mu_B$  versus  $H/T$  plots (Fig. 4) do not superimpose, consistent with the presence of zero field splitting in this molecule. The results observed from this study are not unexpected. It is now firmly established that azido ligands bridging open-shell transition metals in the end-on fashion mediate, almost unvariably, ferromagnetic super-exchange between the spins of the metals. For the cases of  $\text{Cu}^{\text{II}}$  [19] and  $\text{Mn}^{\text{II}}$  [20], correlations between the strength of the coupling,  $J$ , and certain structural parameters have been identified. In the case of  $\text{Ni}^{\text{II}}$ , however, despite the numerous examples reported hitherto [13], it has not been possible to establish such relationship. This issue has been the object of a theoretical study in form of hybrid density functional (DFT) calculations on models consisting of bis-azido bridged dinuclear complexes [21]. For the case of  $\text{Ni}^{\text{II}}$ , a parabolic relationship between the coupling constant and the Ni–N–Ni bridging angle,  $\theta$ , was established for a range of energetically attainable values of  $\theta$ . The coupling was predicted to be ferromagnetic within the entire range, and maximum for the most stable configuration ( $\theta \approx 104^\circ$ ). The ferromagnetic nature of the coupling has been corroborated by the experimental findings from real complexes [7–9,16,22–25]. However, no specific correlation could be identified and the magnitude of the coupling is in all cases approximately half the predicted values. Complex **2** represents a new addition to the list of ferromagnetic complexes of this category. Finding a correlation between the strength of the coupling remains an unsolved challenge which will require consideration of more than one structural parameter at once.

#### 4. Concluding remarks

Reactions of the flexible hexadentate Schiff-base ligand **L** with  $\text{Ni}^{\text{II}}$  has led to the preparation of a mononuclear or a bis-azido bridged dinuclear complex, depending on the presence or not of  $\text{N}_3^-$  ligands in the reaction mixture. The dinuclear complex confirms the feasibility of using complicated multidentate ligands for the preparation and study of dinuclear ( $\mu\text{-N}_3^-$ )-bridged  $\text{Ni}^{\text{II}}$  complexes. In this compound, ferromagnetic super-exchange has been found between the paramagnetic centers, in a magnitude that is consistent with previously found values on compounds displaying analogous structural features.

#### Acknowledgements

The project was supported by grants from the Council of Scientific and Industrial Research New Delhi (Grant No. 01(1836)/03/EMR-II, S.K.C) and the

Department of Science and Technology, New Delhi (Grant No. SR/S1/IC-22/2003, S.K.C.), Government of India, the Malaysian Government and Universiti Sains Malaysia for research (Grant R&D No. 305/PFI-ZIK/610961, H.K.F) and the Spanish Ministry of Science and Technology (“Ramón y Cajal” research contract, GA).

### Appendix A. Supplementary data

Crystallographic data have been deposited with the Cambridge Crystallographic Data Centre, with deposition numbers CCDC 258210 and 258211. Copies of these data can be obtained free of charge on application to CCDC, 12 Union Road, Cambridge CB2 1EZ, UK, fax: +44 1223 336 033, e-mail: deposit@ccdc.cam.ac.uk; or on the web: <http://www.ccdc.cam.ac.uk>. Supplementary data associated with this article can be found, in the online version, at doi:10.1016/j.ica.2005.05.011.

### References

- [1] R.E.P. Winpenny, *Adv. Inorg. Chem.* 52 (2001) 1.
- [2] G. Aromí, S.M.J. Aubin, M.A. Bolcar, G. Christou, H.J. Eppley, K. Folting, D.N. Hendrickson, J.C. Huffman, R.C. Squire, H.L. Tsai, S. Wang, M.W. Wemple, *Polyhedron* 17 (1998) 3005.
- [3] V.A. Milway, L.K. Thompson, D.O. Miller, *Chem. Commun.* (2004) 1790.
- [4] E. Pardo, K. Bernot, M. Julve, F. Lloret, J. Cano, R. Ruiz-García, J. Pasan, C. Ruiz-Perez, X. Ottenwaelder, Y. Journaux, *Chem. Commun.* (2004) 920.
- [5] G. Aromí, P. Gamez, O. Roubeau, H. Kooijman, A.L. Spek, W.L. Driessen, J. Reedijk, *Angew. Chem., Int. Ed.* 41 (2002) 1168.
- [6] G.S. Papaefstathiou, A. Escuer, R. Vicente, M. Font-Bardia, X. Solans, S.P. Perlepes, *Chem. Commun.* (2001) 2414.
- [7] A. Escuer, R. Vicente, S. El Fallah, X. Solans, M. Font-Bardia, *Inorg. Chem. Acta* 247 (1996) 85.
- [8] A. Escuer, R. Vicente, J. Ribas, X. Solans, *Inorg. Chem.* 34 (1995) 1793.
- [9] M.G. Barandika, R. Cortes, L. Lezama, M.K. Urriaga, M.I. Arriortua, T. Rojo, *J. Chem. Soc., Dalton Trans.* (1999) 2971.
- [10] A. Escuer, I. Castro, F. Mautner, M.S. ElFallah, R. Vicente, *Inorg. Chem.* 36 (1997) 4633.
- [11] A. Escuer, R. Vicente, M.S. El Fallah, X. Solans, M. Font-Bardia, *Inorg. Chim. Acta* 278 (1998) 43.
- [12] T.K. Maji, P.S. Mukherjee, G. Mostafa, T. Mallah, J. Cano-Boquera, N.R. Chaudhuri, *Chem. Commun.* (2001) 1012.
- [13] S. Deoghoria, S. Sain, M. Soler, W.T. Wong, G. Christou, S.K. Bera, S.K. Chandra, *Polyhedron* 22 (2003) 257.
- [14] G.M. Sheldrick, 'SHELXS97 Program for Crystal Structure Determination, Göttingen, Germany, 1997.
- [15] G.M. Sheldrick, 'SHELXL97 Program for Crystal Structure Determination, Göttingen, Germany, 1997.
- [16] R. Cortes, J.I.R. Delarramendi, L. Lezama, T. Rojo, K. Urriaga, M.I. Arriortua, *J. Chem. Soc. Dalton.* (1992) 2723.
- [17] A.P. Ginsberg, R.W. Brookes, R.L. Martin, R.C. Sherwood, *Inorg. Chem.* 11 (1972) 2884.
- [18] O. Kahn, *Molecular Magnetism*, New York, 1993, p. 118.
- [19] L.K. Thompson, S.S. Tandon, M.E. Manuel, *Inorg. Chem.* 34 (1995) 2356.
- [20] T.K. Karmakar, B.K. Ghosh, A. Usman, H.-K. Fun, E. Rivière, T. Mallah, G. Aromí, S.K. Chandra, *Inorg. Chem.* 44 (2005) 2391.
- [21] E. Ruiz, J. Cano, S. Alvarez, P. Alemany, *J. Am. Chem. Soc.* 120 (1998) 11122.
- [22] M.I. Arriortua, A.R. Cortes, L. Lezama, T. Rojo, X. Solans, M. Fontbardia, *Inorg. Chem. Acta.* 174 (1990) 263.
- [23] A. Escuer, R. Vicente, J. Ribas, *J. Magn. Magn. Mater.* 110 (1992) 181.
- [24] R. Vicente, A. Escuer, J. Ribas, M.S. Elfallah, X. Solans, M. Fontbardia, *Inorg. Chem.* 32 (1993) 1920.
- [25] J. Ribas, M. Monfort, C. Díaz, C. Bastos, X. Solans, *Inorg. Chem.* 33 (1994) 484.